

A map of the cliff overhang at Stevns Klint

A report for Stevns Kommune in support of coastal hazard assessment at the Stevns Klint UNESCO World Heritage Site

Samuel Paul Jackson, Kristian Svennevig & Erik Vest Sørensen

A map of the cliff overhang at Stevns Klint

A report for Stevns Kommune in support of coastal hazard assessment at the Stevns Klint UNESCO World Heritage Site

Samuel Paul Jackson, Kristian Svennevig & Erik Vest Sørensen

Introduction

Around the Stevns peninsula, a coastal cliff rises for about 14.5 km (Fig.1) to a maximum height of about 40 m, at Stevns Lighthouse (Stevns Fyr). The cliff is a classic Danish geological locality of international relevance and a popular tourist destination, not least since its nomination (Damholt & Surlyk, 2012) and subsequent accession to the UNESCO World Heritage list. For much of its length the cliff has a characteristic undercut profile, resulting from the effect of coastal erosion on the local stratigraphy (Fig. 2). At the base of the cliff, 5–10 m of relatively soft Maastrichtian chalk is overlain by 10–20 m of more resistant Danian limestone. Coastal landslides occur at different scales and frequencies (Pedersen & Strunck, 2011), with seasonal debris shedding being most common. The largest and least frequent landslides involve volumes of the order of 100–1000 m³, and result from failure of the limestone following periods of erosive undermining. Progressive removal of the soft chalk produces increasingly large limestone overhangs, often with sub-horizontal bases that protrude dramatically from the cliff. Members of the public walking along the clifftop have no means of knowing when they are standing on an overhanging section. The overhangs periodically fall onto the beach as cliff slides or rockfalls, posing both an immediate hazard to users of the cliff and a long term challenge to coastal infrastructure planning. These cliff overhangs are the main target of this analysis.

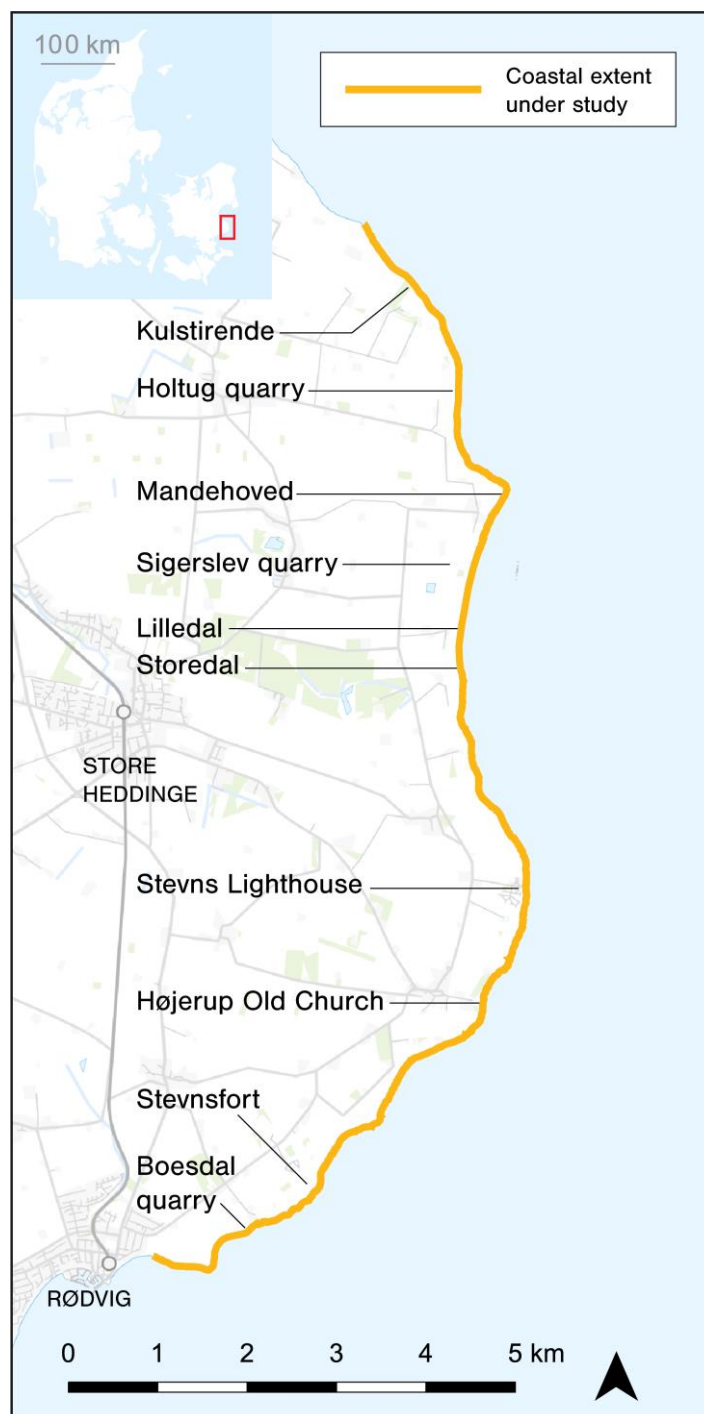


Fig. 1. Area map of the Stevns Peninsula, showing some of the key localities along the coast. The yellow line shows the extent of the photographic coverage that forms the basis of this study.

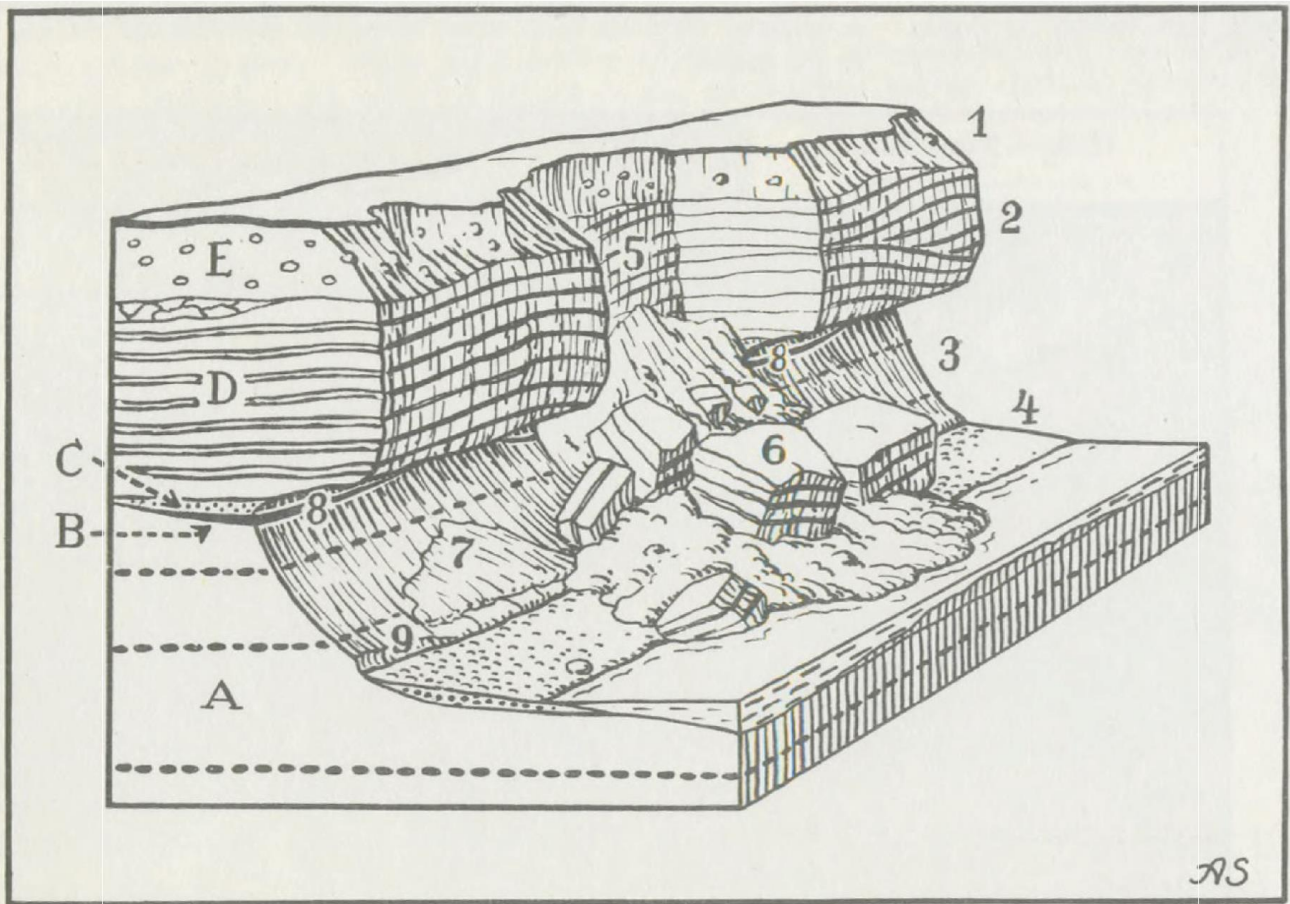
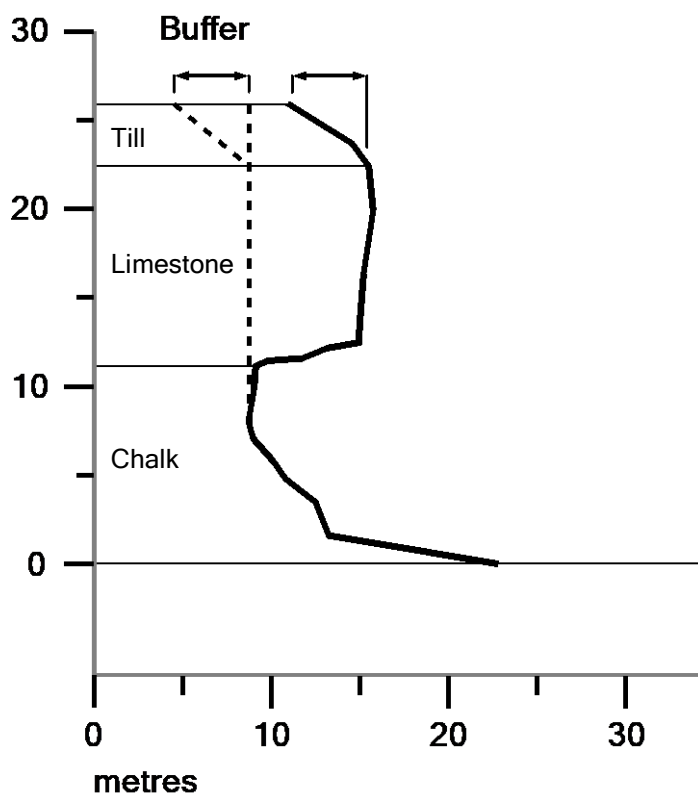


Fig. 2. Axel Schou's 1949 block drawing of the Stevns Klint profile from his 'Atlas over Danmark', concisely capturing its essential features. The view faces north and the block is 30 x 70 m. Note the overhang of the Danian limestone (D) above Maastrichtian chalk (A), and the uppermost till layer (E) with a sloped setback from the top of the limestone. The Cretaceous–Paleogene (K–Pg) boundary runs below the overhang, intermittently following the base of either the limestone or that of the two relatively thin units that occur in small basins: the Fish Clay (B) and Cerithium limestone (C). Note also that the uppermost broken horizontal line depicts the flint band digitized for this study. Schou has included a collapsed section of the cliff, showing a vertical scarp (5) and fallen blocks and scree (6).

the coastline, and particularly to potential revisions to the clifftop path, with the aim of ensuring that the route avoids sections of the clifftop vulnerable to incursion for the next 5–10 years. It builds upon the previous photogrammetric analysis of the coast compiled by Pedersen & Strunck (2011) and owes a debt to the subsequent detailed field descriptions of Pedersen & Gravesen (2016).

Our approach has been to map and quantify the area of the cliff overhangs. We did this by means of a photogrammetric analysis of a new series of images of the coastline and subsequent GIS (Geographic Information System) analysis. From our images we digitized 3D polylines that trace the undercut and overhanging parts of the cliff. By projecting these vertically and intersecting them with each other we generated a set of polygons which show, in map view, the shape and location of overhangs along the coast. In addition, we have considered the potential landward incursion of landslides beyond the overhanging sections. The limestone cliff is overlain by a glacial till layer of variable thickness. Observation of the coast indicates that when overhangs fail, they initially leave a near-vertical scarp of limestone and till, but that over

subsequent seasons the till layer recedes further, resulting in a sloped setback from the top of the limestone (Fig 3). We have incorporated this loss of till cover in our map as a buffer, to better reflect the full potential encroachment of landslides (Fig. 4).



Above: Fig. 3. A section of the cliff illustrating the development of a setback in the till at the top of the cliff. On the left, a relatively fresh landslide has produced a near-vertical scarp in both the limestone and the till. At bottom left landslide debris lies on the beach. At top right, the common configuration of the clifftop – a sloped setback of the till, often colonised by vegetation. The height shown is approximately 25 m.

Left: Fig. 4. A profile of Stevns Klint digitised from the cliff immediately north of Højerup with a schematic depiction of geological units. The vertical dashed line traces upwards from the deepest undercut point, while the oblique line represent the additional setback in the till layer, which we have modelled as a buffer.

Methods

Polyline digitisation

The digitisation of the cliff was carried out following the established workflow of the Photogeological Laboratory at GEUS. We took a sequence of photographs of Stevns Klint from a small boat sailing alongshore at a distance of about 100 m. The coverage begins immediately north-east of Rødvig harbor and ends at the headland 1.5 km south-east of Bøgeskov harbor, where the cliff gives way to a lower coastal profile. The sequence comprises some 1080 photographs, and closely matches the extent that was profiled by Surlyk et al. (2006). We brought the images into the Photogeological Laboratory and prepared them as a sequence of connected stereo models, in which the relative image orientation is obtained via automatic comparison of landmarks in the overlapping portions of image pairs, with subsequent manual refinement as necessary. Real coordinates are introduced by means of a camera-mounted GNSS receiver and ground control points. The technical details of the method are described by Sørensen and Dueholm (2018). Once set up, the stereo images formed the canvas for 3D digitization of geological features, which we drew as polylines directly onto the images at a dual-monitor stereo workstation.

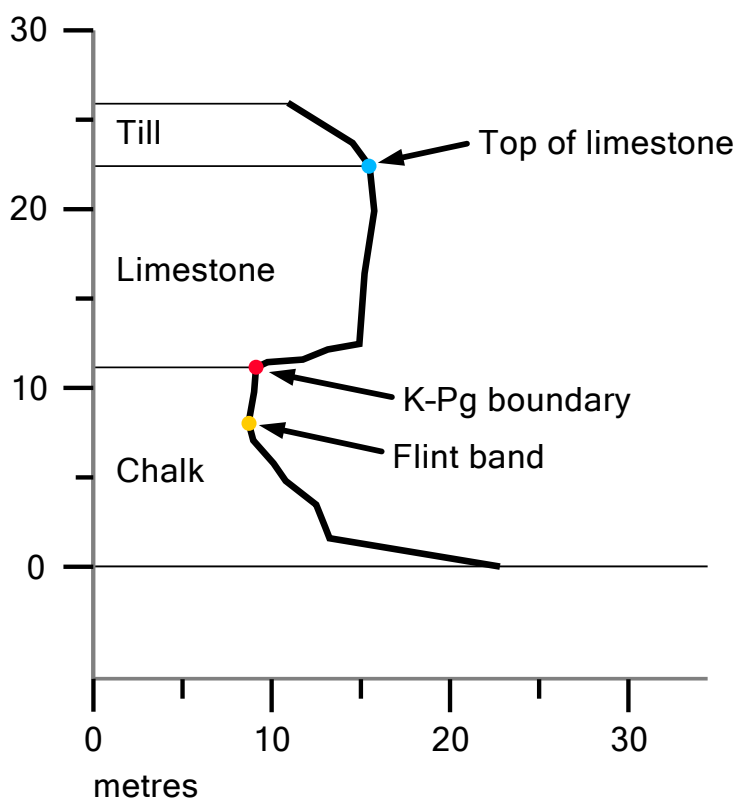


Fig. 5. Cliff profile indicating three of the features selected for digitisation. A fourth class of line was used where neither of the two undercutting features shown above could be traced.

To capture the cliff overhang, we traced the deepest undercut part of the cliff as well as the furthest protrusion. To do so efficiently, we selected proxy geological and geomorphological features that could be followed reliably over long stretches of the coastline (Figs. 5 and 6). The Cretaceous–Paleogene (K–Pg) boundary occurs at the junction of the chalk and limestone, and for much of the coast corresponds to the most deeply undercut horizon. A prominent dark flint band, some 5 m lower on the cliff, within the Maastrichtian chalk, is occasionally cut even more deeply than the K–Pg boundary. At almost any place where there are overhangs, one or other of these horizons is at, or very near, the deepest point. A separate class of polyline was digitised on the few sections where neither of these horizons is exposed, but where an undercut nonetheless

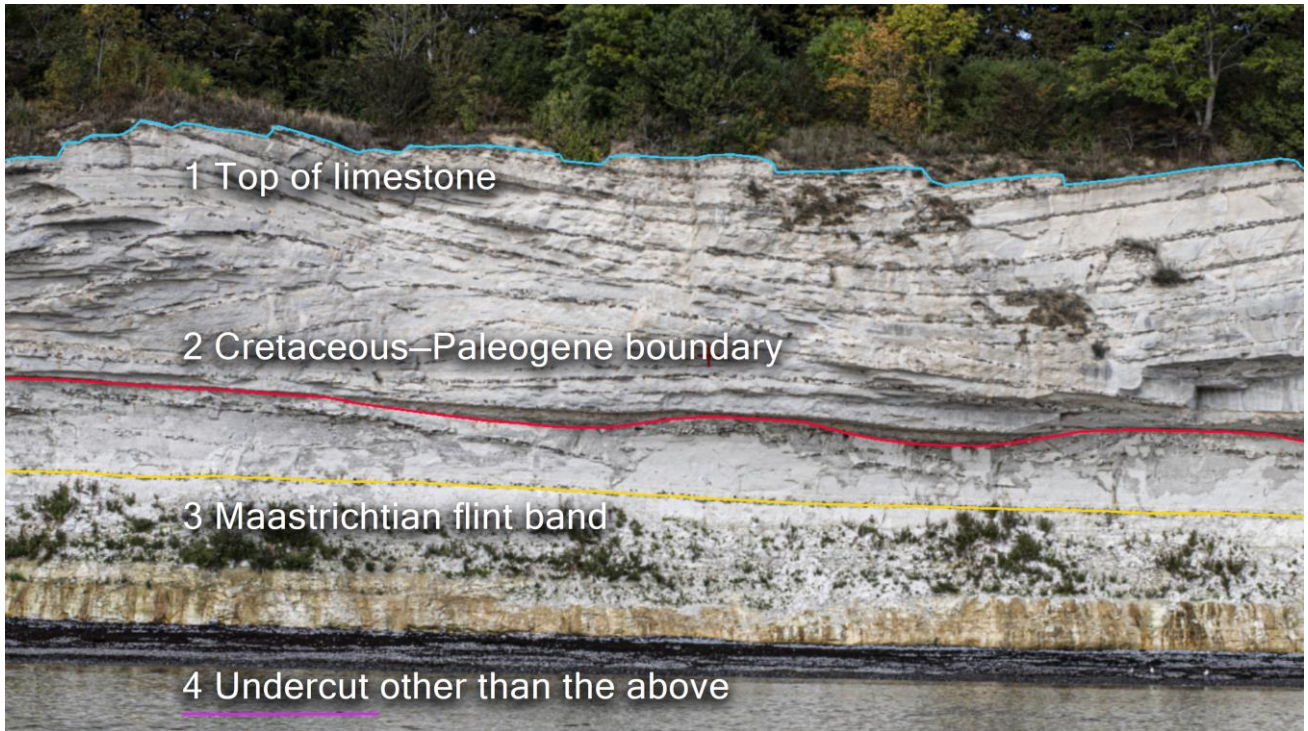


Fig. 6. The four features digitised in this analysis, of which the first three are shown in position on the cliff face. This image, minus labels, is captured directly from the stereo workstation and shows a flat version of the main working view used in the digitisation process.

exists. This mostly pertains to a small section of cave-eroded coastline north of Boesdal quarry. This final class of undercut line does not trace a geological horizon but was digitised solely by stereo depth estimation. To capture the seaward reach of the overhang, we traced the visual top of the Danian limestone. This is treated as a geomorphological, rather than a geological feature, since the actual contact surface with the till is generally obscured. It should also be noted that the limestone face is in places convex, such that a lower part projects outward yet further. The top is nonetheless a good proxy that has the advantage of being consistently traceable along almost the entire coastline. The digitisation process produces a 3D dataset of categorised polylines (Fig. 7).

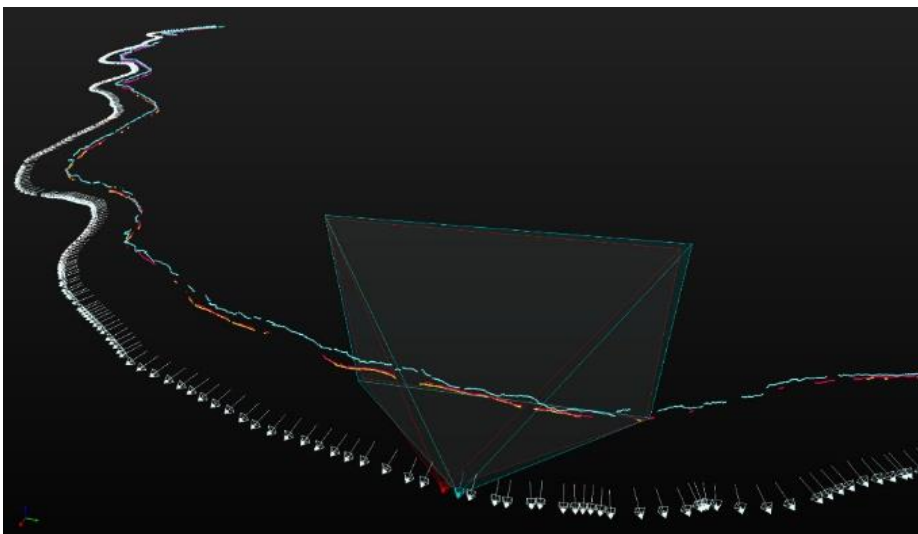


Fig. 7. A view of the 3D polyline data for Stevns Klint from the stereo workstation. The white objects mark camera positions. In this screenshot, the viewing frustum is centred in the vicinity of Stevns Lighthouse. The left of the image shows the coastline stretching southwards towards Højerup and beyond.

Buffer estimation

To calculate the buffer used to represent the post-landslide till slope, we measured the shape of the present slope at intervals of approximately 200 m, excluding sections lacking a limestone cliff or where the slope was obscured by vegetation. Specifically, we placed 58 two-point polylines extending from the top of the limestone to the top of the till slope (Fig. 8). We extracted the elevation values of the two vertices and subtracted them to give an estimate of the till thickness. We used a conservative angle of 45 degrees, shallower than the measured mean of 52 degrees, to trigonometrically calculate the landward reach of the slope.

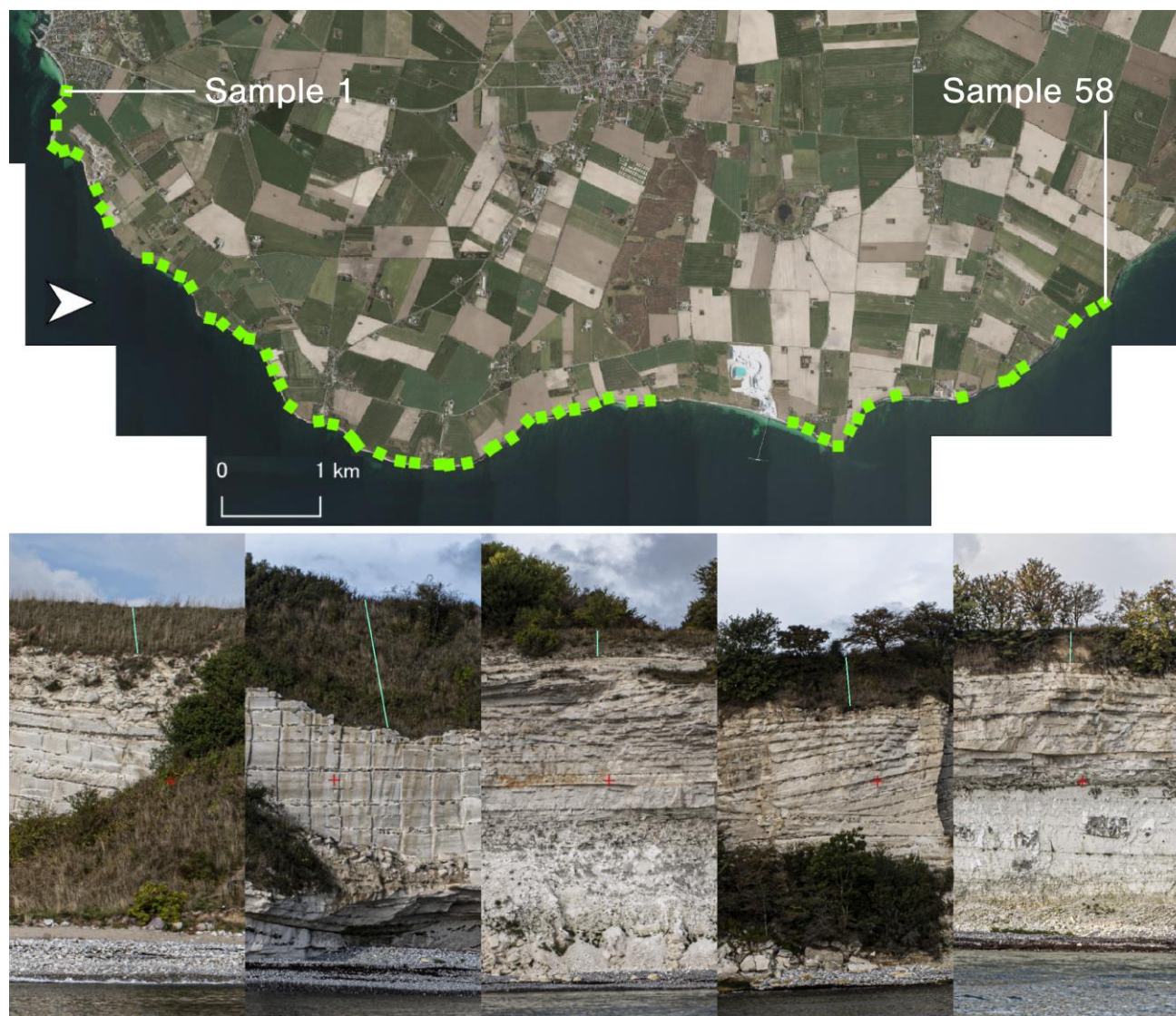


Fig. 8. Map of locations at which the till slope was measured for the purpose of calculating an appropriate buffer, with selected images from the stereo view to illustrate the sampling method. The table of measurements is supplied in Appendix A.

GIS analysis

We exported the digitized polylines from the stereophotogrammetry workflow and transferred them into GIS (QGIS) as shapefiles (.shp). We first tidied the polylines by bridging small gaps (generally smaller than 100 m) and manually removing small loops and kinks. We applied light smoothing to improve the cartographic appearance of the lines. When mapped, the four digitised line features intersect each other along the coast as dictated by the profile of the cliff (Fig. 9).

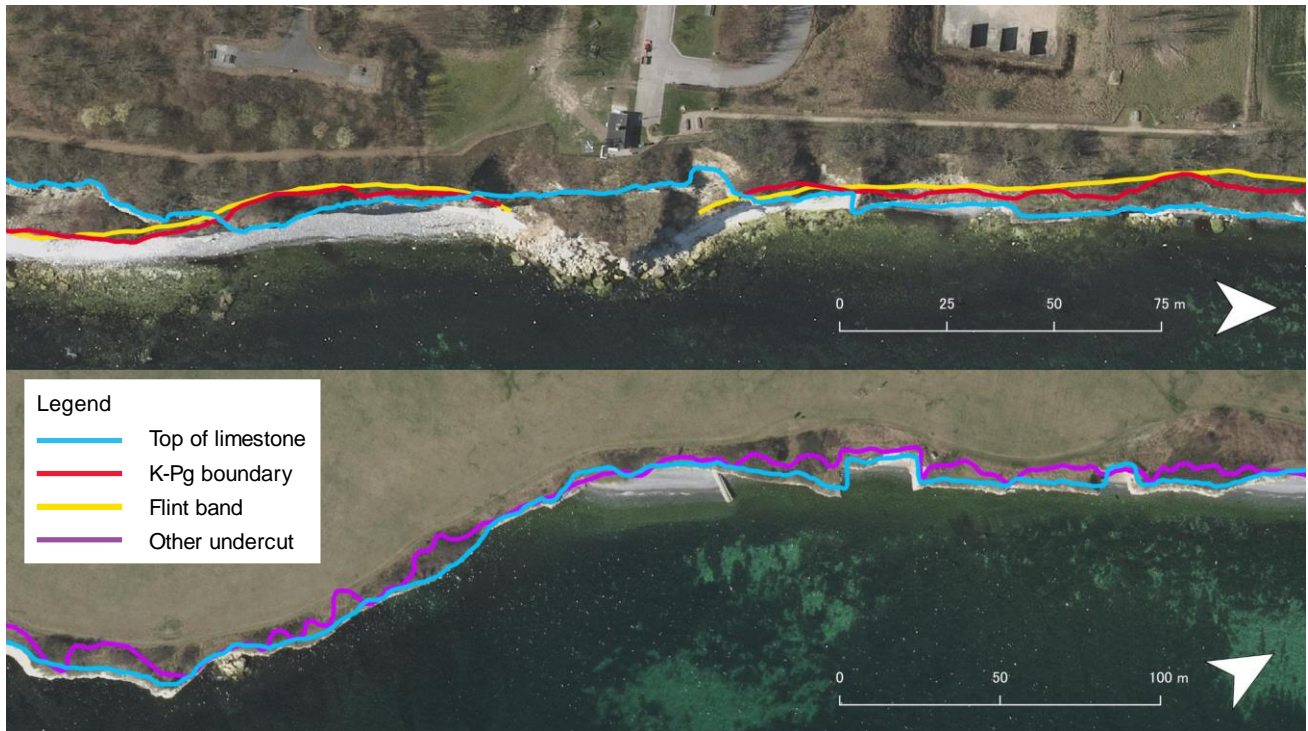


Fig. 9. Two views of the polyline data following mapping in GIS software, from Stevns Lighthouse (above) and Stevnsfort respectively. At the lighthouse, the top limestone line alternates with the two lines representing the undercut. Note the discontinuous nature of the digitised lines, in this instance due to landslide debris under the viewing point concealing the lower part of the cliff succession. At Stevnsfort, the K-Pg boundary lies too low to be traced, so this part of the coast provides an example of somewhere the undercut was judged by visual depth estimation to be the deepest point. Note the rectangular recess in the cliff, right of centre, a common tell-tale sign of former small-scale coastal quarrying.

The overlapping areas where the top of the limestone extends further outwards towards the sea than the undercutting lines indicate an overhanging section of cliff, while the opposite overlap indicates a cliff profile leaning landwards or containing a bench. To highlight the overhang, we generated polygons covering all of the first type of overlap (Fig. 10).

Following the measurements arrived at by sampling the till (Appendix A), we generated buffers on the landward side of all four lines. We then merged these into a single buffer that consequently follows whichever line is closest to land. That is to say, the buffer runs at a minimum parallel to the top of the limestone but diverges landwards from it where overhangs occur.

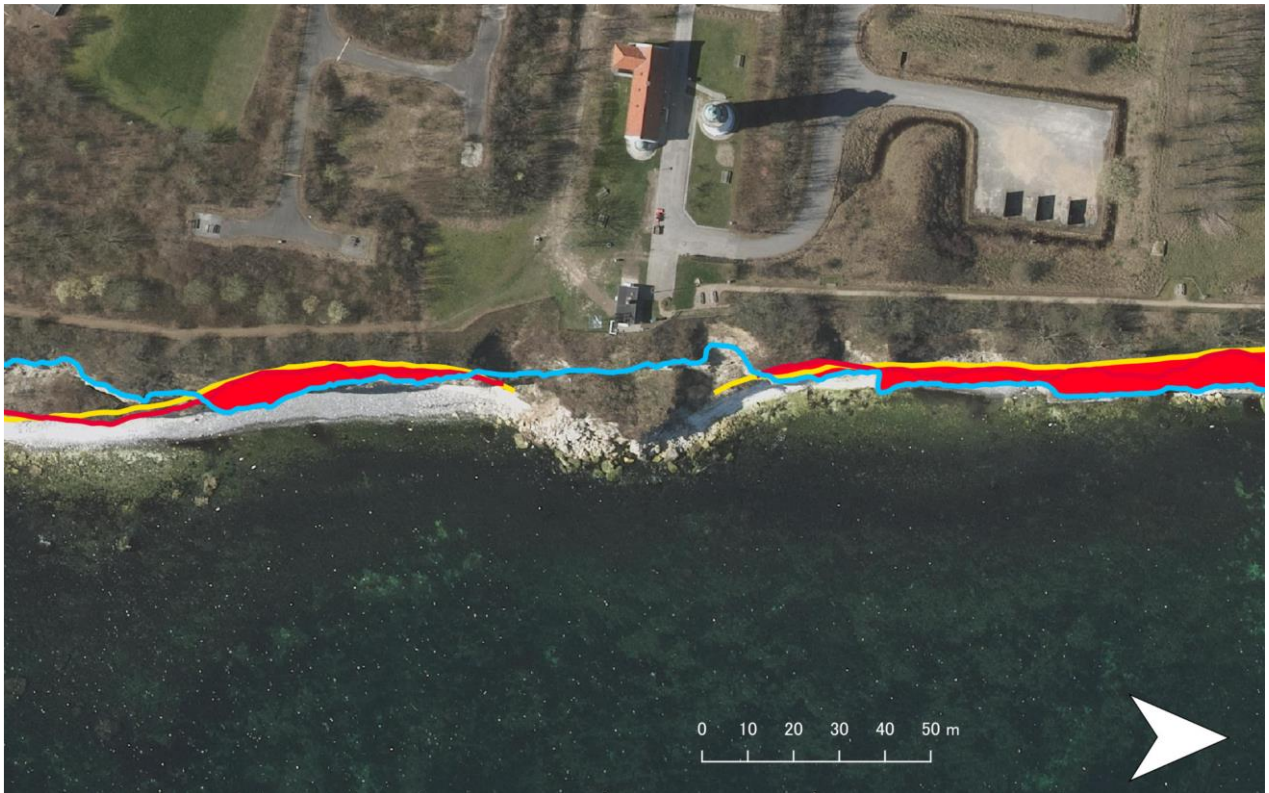


Fig. 10. Overlap polygons generated from the polylines in the vicinity of Stevns Lighthouse. This particular section illustrates a pattern observed in several places along the coastline, in which current overhangs alternate with former landslides.

Results

Our analysis generated 230 cliff overhang polygons, with a combined area of 21431.42 m² (for comparison, a standard association football pitch measures 7140 m²). A large number of these overhangs are trivially small. Only 167 have an area greater than 1 m², and these collectively capture 99.92% of the total overhang area. The largest 15 overhangs capture 49.88% of the total area. An overview of the distribution of overhangs is shown in Fig. 11. The full map data are appended in digital format.

The measurements of the till slope indicate that the till is relatively thick in the centre of the cliff, and thinner at its northern and southern ends. The calculated potential incursion of the till slope varies according to till thickness, for which reason we propose three classes of buffer, namely: 5 m for the majority of the coast, 10 m for an inner 5 km stretch, from Harvig to Storedal, and 15 m for a 1.5 km stretch between Stevns Lighthouse and Barmhertigheden. An average rate of erosion of 15 cm/yr was previously estimated by Pedersen & Gravesen (2011) from comparison of the mapped coastlines in 1891 and 2010. Multiplying this by 5 years, which is the expected period between hazard assessments, gives 75 cm, which we added to our buffer for final values of 5.75 m, 10.75 m, and 15.75 m.

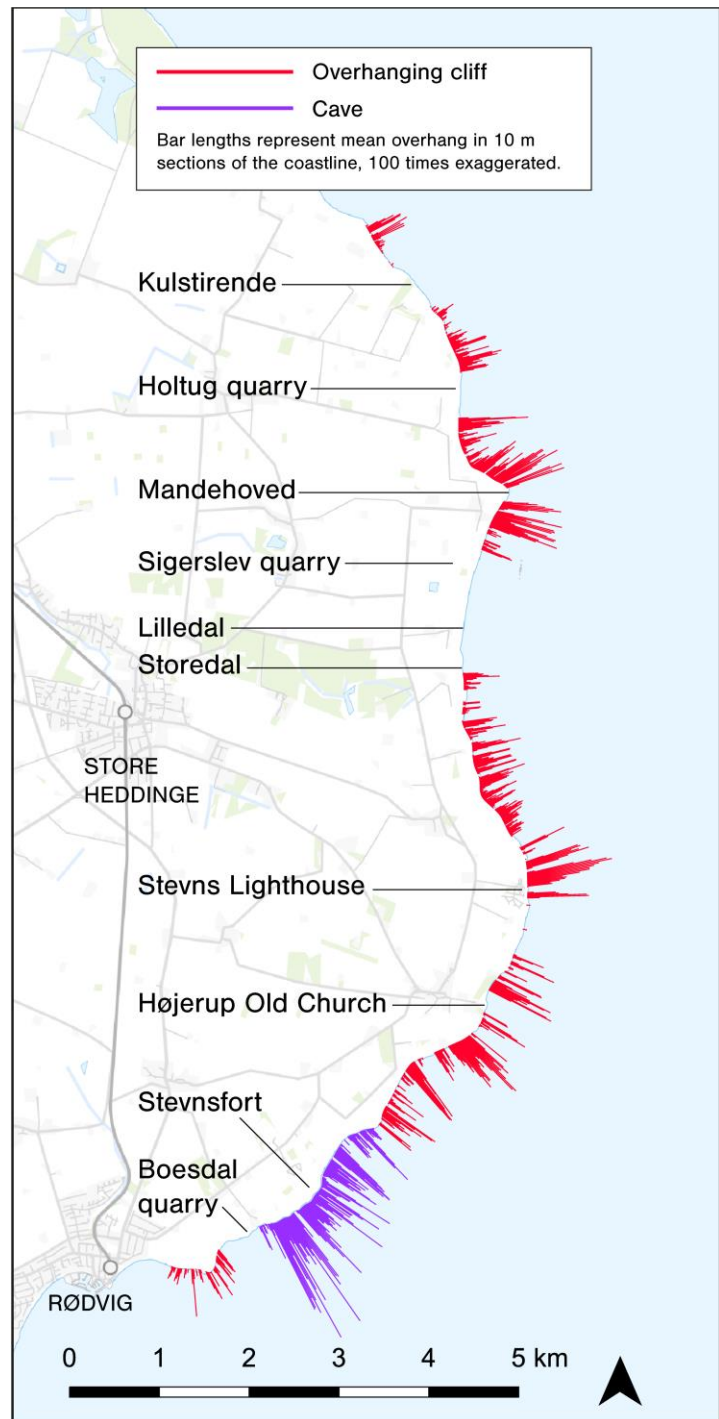


Fig. 11. Representation of the overhang distribution along the Stevns coastline. Bars were generated as a 100x exaggeration of the overhang within 10 m-wide slices of the coastline. A section of caves north of Boesdal quarry is categorised separately from the more typical cliff overhang. Excepting the quarries, overhangs are remarkably ubiquitous. The deepest overhangs frequently extend about 8–10 m over the beach.

Distribution and types of overhang

By far the predominant form of overhang is the notch-cut limestone-over-chalk type. This form of cliff morphology characterizes those parts of the coast where the K-Pg boundary horizontally bisects the cliff. This is the case for most of the coastal extent, with the consequence that such overhangs are widespread. This form of overhang is typically much wider than deep, extending often to 100 m or more in width while rarely exceeding about 8 m in depth, and only exceptionally approaching 10 m. Some unusually narrow protrusions do occur, and this is generally as a result of historic small-scale quarrying activity having modified the cliff profile. Areas with particularly deep overhangs occur to the immediate north and south of Højerup Old Church, the immediate north of Stevns Lighthouse, and on either side of the headland at Mandehoved.

Conversely, this type of overhang is largely absent along those parts of the coast where the K-Pg boundary is not exposed, either because it runs below sea level or above cliff level. The only portion of the coastline in which the boundary runs below sea level is a 2 km long stretch running from Boesdal quarry northwards past the location of Stevnsfort. Here it is limestone, rather than chalk that is exposed to erosion at sea level. The relatively hard limestone shows a distinct erosional pattern, essentially limited to this stretch of coast, namely the carving of deep but relatively narrow caves under the cliff. Some of these caves exceed 15 m in depth, thus greatly exceeding the depth of overhang seen elsewhere on the coastline. We hypothesise that a key factor may be that the cave overhangs have roughly $\frac{3}{4}$ lateral contact with the adjoining limestone beds, compared to between $\frac{1}{2}$ and $\frac{1}{4}$ in the case of cliff overhangs, and the limestone may therefore be subject to a more uniform stress distribution. We also conjecture that the mounded bedforms of the limestone might confer some additional resistance to collapse by forming natural arches. Either the first or both of these conditions could explain why overhangs can form to a greater depth here than elsewhere.

Where the K-Pg boundary exceeds the height of the cliff the entire face is composed of Maastrichtian chalk and overlying Quaternary till. This is the case between Storedal and Sigerslev quarry, and in a stretch either side of Kulstirende, for a combined extent of about 2 km. This cliff configuration probably suppresses the formation of a significant overhang due to the lack of contrast in strength between layers. In such instances cliff erosion is more heavily dominated by smaller-continual erosion, which nonetheless can occur at significant overall rates (Pederen & Gravesen, 2016). These sections are neither amenable to the present methodology nor do they present an overhang hazard of the type seen elsewhere along the coast, and are thus omitted from the scope of this analysis.

Smaller breaks in the overhang are found immediately behind former landslides occupying the beach, which provide as a temporary defence against erosion, such as occurs immediately south of Stevns Lighthouse. Some degree of protection is also given by the benches of the many small limestone quarries that are scattered along this coast. The very same quarries, however, produce exposed corners at either ends of their width, which themselves can in fact promote the development of prominent angular overhangs once the chalk beneath becomes subject to erosion.

A close overall relationship exists between the presence and type of overhang, and the position of the K-Pg boundary on the cliff (c.f. the topographic profile of Lykke-Andersen & Surlyk, 2004).

Limitations and future directions

The total overhang area of 21431.42 m² measured by this study is necessarily an underestimate, due the fact that during the manual tracing of features, any deviation from either the deepest or the most projecting horizons can only result in a lower, not higher intersection area. It is likely that the very deepest part of the undercut was not reached at every point. Likewise, the top of the limestone is not always the most extreme prominence of the cliff face. An average under-measurement, for instance, of 10% of the depth of the overhang would imply a total area of approximately 23813 m². A different treatment of the data, namely modelling the entire cliff as a 3D polyhedron, could potentially overcome this issue, but would be a more complex undertaking than the present analysis.

The workflow used here offers the possibility of a relatively quick turnaround time from data acquisition to mapping. This first quantification of the overhang area provides, however, only a static view of the condition of the coastline. Future analyses following the same workflow would allow comparison across time, and thus provide a better insight into the changing condition of the coastline. This could greatly improve the understanding of erosion patterns, and hence further refine the focus in respect of safety considerations.

Conclusion

The analysis of the Stevns Klint indicates that overhangs occur frequently throughout almost the entire 14.5 km extent of the coastline. The few exceptions occur where the cliff is wholly composed of soft chalk and till, as between Storedal and Lilledal and in the vicinity of Kulstirende. In general, the variable elevation of the K-Pg boundary heavily influences the type of erosion at any given location. The three larger coastal quarries (Boesdal, Sigerslev and Holtug) create interruptions in the cliff and hence the overhang. The small abandoned quarries interspersed along the cliff tend to create benches which insulate the cliff behind them from coastal erosion, but exacerbate the prominence of sections of the cliff lateral to them. Past landslides occupying the beach similarly inhibit the development of overhang in the cliff behind while they persist. This is most clearly in effect in the relatively overhang-free interval immediately south of Stevns Lighthouse. Exceptionally deep undercutting of the cliff occurs in the cave-eroded section of coastline north of Boesdal quarry, which we speculate are permitted to develop to such depths by the presence of relatively hard limestone at sea level and the geometry of the caves. If the caves are excluded, the depth of overhang tops out fairly consistently at 8–10 m. A relatively thick till layer in the central portion of the coastline probably implies a greater potential for landward incursion of landslides, which we have reflected in our buffer estimations.

Photogrammetric digitisation combined with GIS analysis offers an efficient way of capturing the overhang of the coastal cliff. The method is readily scalable and replicable, and further such analyses would provide a valuable source of comparative data.

References

Damholt, T. & Surlyk, F. 2012: Nomination of Stevns Klint for inclusion in the World Heritage List.

Østsjælland Museum.

Lykke-Andersen, H., & Surlyk, F. 2004: The Cretaceous-Paleogene boundary at Stevns Klint, Denmark: Inversion tectonics or sea-floor topography?
Journal of the Geological Society, 161, 343-352.

Pedersen, S.A.S. & Strunck, M.N. 2011: Vurdering af fjeldskredsrisko på Stevns Klint.
Danmarks og Grønlands Geologiske Undersøgelse Rapport 2011/93.

Pedersen, S.A.S. & Gravesen, P. 2016: Risikovurdering af skredforhold langs Stevns Klint.
Danmarks og Grønlands Geologiske Undersøgelse Rapport 2016/33.

Schou, A. 1949: Atlas over Danmark, I: Landskabsformene.
Det Kongelige Danske Geografiske Selskab. Hagerup, København.

Surlyk, F., Damholt, T. & Bjerager, M. 2006: Stevns Klint: Uppermost Maastrichtian chalk, Cretaceous-Tertiary boundary, and lower Danian bryozoan mound complex.
Bulletin of the Geological Society of Denmark 54, 1-48.

Sørensen E. V., & Dueholm, M. 2018: Analytical procedures for 3D mapping at the Photogeological Laboratory of the Geological Survey of Denmark and Greenland.
GEUS Bulletin, 41, 99-104.

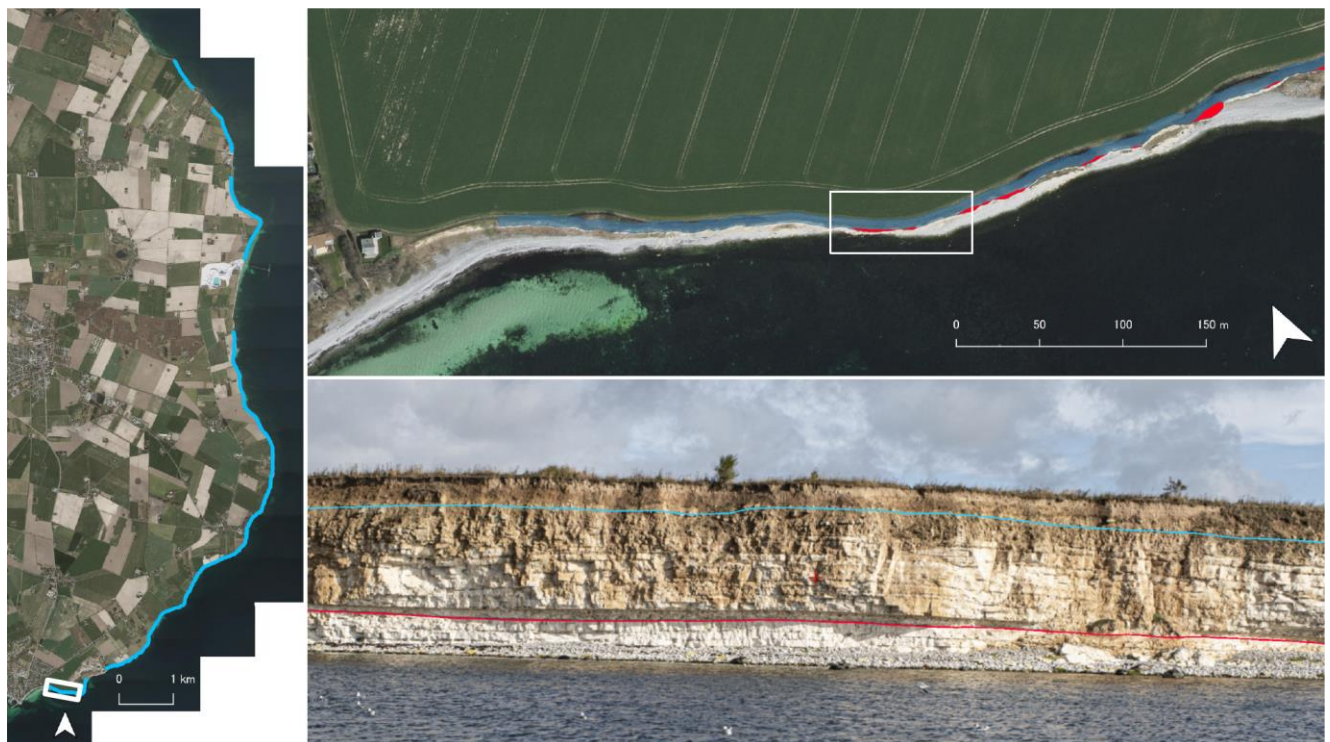
Appendices

Appendix A: Table of buffer calculations







Two-point slope polylines		First point coordinate			Second point coordinate			Z difference (proxy for fill thickness) and angle		Calculated buffers (m)		Using mean angle		Using 45 degrees (const)		Suggested buffer		Approximate location	
Geometry ID		x	y	z	x	y	z	Z difference (m)	Dip angle (degrees)	Using variable angle									
1	Polyline2021111608532401	715197.96	6128452.41	11.46	715197.65	6128450.00	7.37	59.3	4.09	59.3	2.43	3.13	4.09	575	Redvig				
2	Polyline2021111608532402	715364.64	6128373.75	13.09	715363.60	6128372.81	10.55	61.2	2.54	61.2	1.40	1.94	2.54	575					
3	Polyline2021111608532403	715574.25	6128338.83	14.74	715574.27	6128338.12	13.10	66.6	1.63	66.6	0.71	1.25	1.63	575					
4	Polyline2021111608532404	715816.77	6128314.30	17.37	715818.72	6128312.92	14.20	53.0	3.17	53.0	2.39	2.43	3.17	575					
5	Polyline2021111608532405	715856.76	6128421.53	18.12	715861.35	6128422.54	13.35	45.5	4.77	45.5	2.69	3.65	4.77	575					
6	Polyline2021111608532406	715892.38	6128570.19	19.67	715894.76	6128568.99	16.92	46.0	2.76	46.0	2.66	2.11	2.76	575					
7	Polyline2021111608532407	716295.48	6128782.80	18.09	716286.86	6128780.00	14.58	48.3	3.50	48.3	3.12	2.68	3.50	575	Boesdal				
8	Polyline2021111608532408	716486.40	6128843.32	15.41	716486.99	6128840.06	9.03	56.0	6.37	56.0	4.30	4.87	6.37	575					
9	Polyline2021111608532409	716841.78	6128915.58	16.88	716842.69	6128912.13	12.25	52.4	3.57	52.4	3.57	3.55	4.64	575					
10	Polyline2021111608532410	717042.77	6129350.15	16.30	717044.67	6129350.08	13.86	52.2	2.44	52.2	2.65	1.87	2.44	575					
11	Polyline2021111608532411	717122.91	6129517.80	17.67	717125.36	6129516.79	14.58	53.0	3.09	53.0	3.96	2.36	3.09	575					
12	Polyline2021111608532412	717242.38	6129708.36	18.53	717246.17	6129707.22	13.28	53.0	5.25	53.0	4.92	4.02	5.25	575					
13	Polyline2021111608532413	717360.66	6129826.09	21.01	717363.18	6129821.88	15.02	50.6	5.99	50.6	4.92	4.58	5.99	575					
14	Polyline2021111608532414	717703.63	6130038.56	23.45	717713.45	6130036.38	14.66	41.1	8.79	41.1	10.07	6.72	8.79	1075					
15	Polyline2021111608532415	717722.84	6130180.42	23.95	717715.53	6130177.92	19.69	49.3	4.27	49.3	3.67	3.26	4.27	1075					
16	Polyline2021111608532416	717871.19	6130369.14	24.89	717875.34	6130365.59	18.15	51.0	5.46	51.0	5.46	5.16	6.74	1075					
17	Polyline2021111608532417	717930.69	6130473.37	24.95	717935.19	6130472.73	19.00	52.6	5.94	52.6	4.54	4.54	5.94	1075	Harvig				
18	Polyline2021111608532418	718109.64	6130687.65	27.81	718111.46	6130683.43	19.74	60.3	8.07	60.3	4.61	6.17	8.07	1075					
19	Polyline2021111608532419	718276.30	6130737.55	27.08	718278.28	6130731.81	19.89	49.8	7.19	49.8	6.07	5.49	7.19	1075					
20	Polyline2021111608532420	718441.63	6130818.36	26.90	718444.25	6130812.96	20.22	48.1	6.68	48.1	5.99	5.11	6.68	1075					
21	Polyline2021111608532421	718679.76	6130939.37	28.32	718684.25	6130936.23	20.90	53.6	7.42	53.6	5.47	5.47	7.42	1075	Hejrup				
22	Polyline2021111608532422	718873.65	6131238.31	26.82	718884.52	6131238.85	20.86	50.8	5.97	50.8	4.90	4.56	5.97	1075					
23	Polyline2021111608532423	718879.82	6131387.22	25.66	718881.38	6131386.90	23.71	50.8	1.96	50.8	1.60	1.50	1.96	1075					
24	Polyline2021111608532424	719016.39	6131669.92	26.39	719019.33	6131663.78	21.38	49.4	5.01	49.4	4.30	3.83	5.01	1075					
25	Polyline2021111608532425	719107.98	6131869.19	28.93	719110.60	6131865.70	24.04	48.3	4.89	48.3	4.35	3.74	4.89	1075					
26	Polyline2021111608532426	719200.89	6131915.55	32.11	719206.93	6131912.73	26.27	41.2	8.84	41.2	6.67	4.47	8.84	1075					
27	Polyline2021111608532427	719282.15	6132141.73	35.35	719290.45	6132140.32	27.15	58.0	5.60	58.0	1.01	1.01	5.60	1075					
28	Polyline2021111608532428	719305.11	6132288.32	37.83	719306.11	6132288.19	32.23	79.8	5.08	79.8	1.01	1.01	5.60	1075	Stevns fyr				
29	Polyline2021111608532429	719319.10	6132572.77	40.27	719324.17	6132573.01	32.48	56.9	7.79	56.9	11.16	7.79	7.79	1075					
30	Polyline2021111608532430	719321.46	6132677.13	40.09	719332.55	6132678.52	30.14	41.7	9.95	41.7	11.61	9.89	9.95	1075					
31	Polyline2021111608532431	719303.78	6132879.18	38.06	719313.15	6132881.26	25.13	53.4	12.93	53.4	9.61	8.89	12.93	1575					
32	Polyline2021111608532432	719152.21	6133131.59	35.52	719155.63	6133134.65	30.33	48.5	5.18	48.5	4.59	4.59	5.18	1575					
33	Polyline2021111608532433	719125.77	6133182.88	35.92	719123.73	6133185.46	30.34	50.6	5.59	50.6	4.59	4.27	5.59	1575					
34	Polyline2021111608532434	719025.77	6133369.53	35.19	719033.81	6133375.04	25.18	45.8	10.01	45.8	9.74	7.66	10.01	1575					
35	Polyline2021111608532435	718839.68	6133545.18	36.06	718844.91	6133550.35	26.13	53.5	9.93	53.5	7.35	7.59	9.93	1575	Tommestrup				
36	Polyline2021111608532436	718797.64	6133697.33	39.14	718803.48	6133698.34	26.96	64.1	12.18	64.1	5.92	6.94	12.18	1575					
37	Polyline2021111608532437	718742.89	6133889.71	37.90	718748.64	6133893.33	28.82	53.2	9.08	53.2	6.79	6.94	9.08	1575					
38	Polyline2021111608532438	718706.76	6134064.10	37.81	718722.20	6134065.87	22.32	44.9	15.48	44.9	15.54	11.84	15.48	1575	Barnhøjheden				
39	Polyline2021111608532439	718653.79	6134287.01	39.67	718659.69	6134289.80	31.93	49.8	7.74	49.8	6.54	5.91	7.74	1075					
40	Polyline2021111608532440	718595.85	6134436.97	40.57	718595.14	6134438.15	32.06	57.5	8.50	57.5	5.42	6.50	8.50	1075					
41	Polyline2021111608532441	718622.56	6134684.52	38.12	718625.17	6134684.77	33.10	62.4	5.02	62.4	2.62	3.83	5.02	1075					
42	Polyline2021111608532442	718616.27	6134903.11	35.88	718620.00	6134903.24	29.58	59.4	6.31	59.4	3.73	4.82	6.31	1075	Storødal				
43	Polyline2021111608532443	718556.03	6136480.22	37.61	718559.65	6136479.72	34.38	41.5	3.23	41.5	3.65	2.47	3.23	575					
44	Polyline2021111608532444	718929.03	6136645.84	34.11	718932.12	6136644.61	31.20	49.7	2.91	49.7	2.02	2.22	2.91	575					
45	Polyline2021111608532445	719040.08	6136822.29	31.24	719041.97	6136821.58	28.85	41.2	2.39	49.7	3.32	1.82	2.39	575	Mandelhøved				
46	Polyline2021111608532446	719116.68	6136978.86	30.17	719119.34	6136978.86	28.20	36.4	1.97	36.4	2.67	1.50	1.97	575					
47	Polyline2021111608532447	718941.31	6137108.76	27.47	718942.82	6137111.74	23.98	46.2	3.49	46.2	3.35	2.67	3.49	575					
48	Polyline2021111608532448	718814.49	6137198.15	25.74	718814.96	6137199.75	23.52	53.3	2.22	53.3	1.66	1.70	2.22	575					
49	Polyline2021111608532449	718673.14	6137309.24	25.74	718674.67	6137310.02	23.09	58.8	2.84	58.8	1.72	2.17	2.84	575					
50	Polyline2021111608532450	718560.11	6137616.51	28.81	718563.05	6137617.19	25.16	50.5	3.65	50.5	3.01	2.79	3.65	575					
51	Polyline2021111608532451	718577.87	6138347.78	24.66	718580.17	6138348.27	22.79	38.4	1.87	38.4	2.36	1.43	1.87	575	Høllug				
52	Polyline2021111608532452	718405.62	6138814.07	19.85	718406.24	6138814.18	17.64	74.1	2.21	74.1	0.63	1.69	2.21	575					
53	Polyline2021111608532453	718358.80	6138906.15	19.09	718361.86	6138908.89	14.03	50.9	5.06	50.9	4.11	3.87	5.06	575					
54	Polyline2021111608532454	718250.24	6139017.74	17.15	718252.62	6139019.15	18.01	48.7	3.14	48.7	2.76	2.40	3.14	575					
55	Polyline2021111608532455	717858.63	6139437.99	19.85	717858.68	6139438.12	14.04	85.6	1.81	85.6	0.14	1.38	1.81	575	Kulstrenden				
56	Polyline2021111608532456	717734.00	6139598.20	21.88	717734.42	6139598.66	20.73	61.6	1.16	61.6	0.63	0.88	1.16	575					
57	Polyline2021111608532457	717611.64	6139783.26	23.40	717612.55	6139783.78	20.96	66.4	2.42	66.4	1.06	1.85	2.42	575					
58	Polyline2021111608532458	717535.09	6139919.22	18.82	717537.92	6139921.39	15.34	44.3	3.48	44.3	3.57	2.66	3.48	575					
Mean dip angle →										52.6									

Appendix B: Selected localities

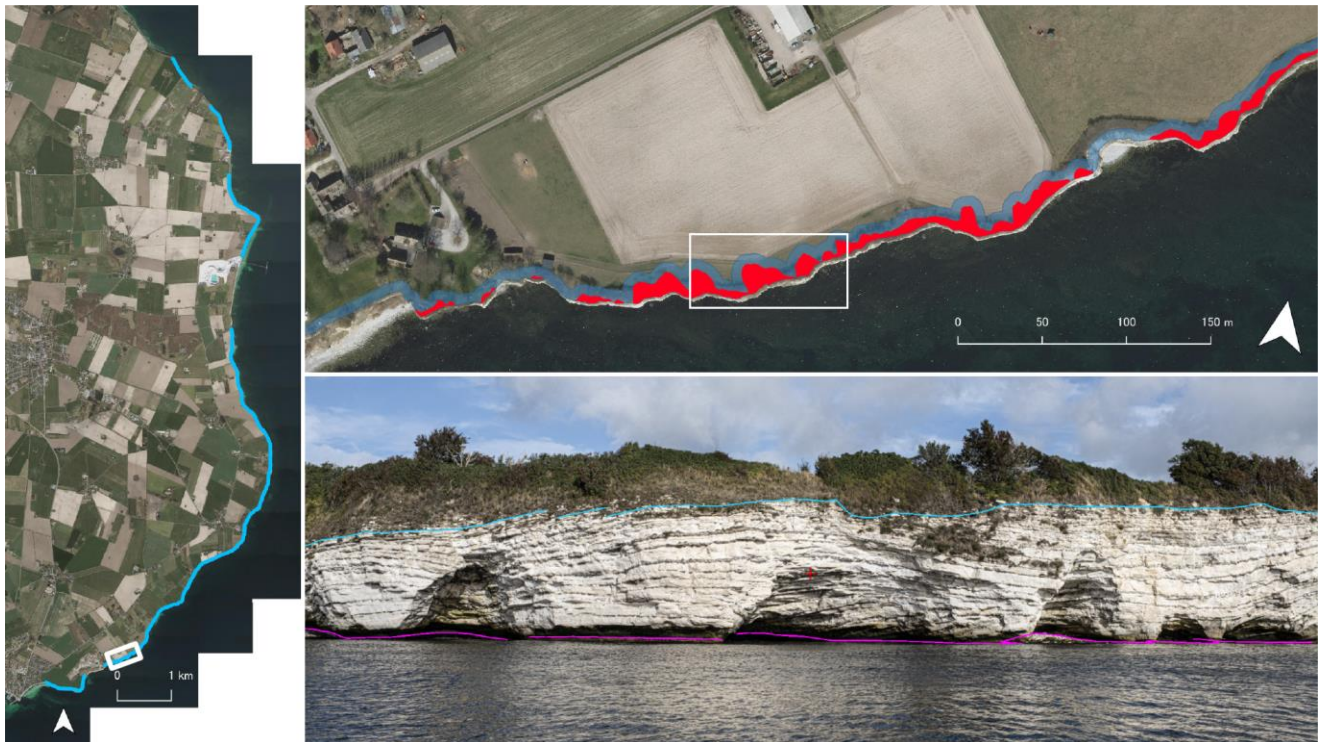
Rødvig



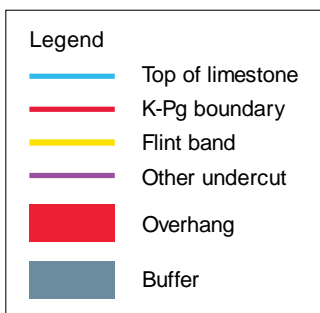
A small overhang first appears within a few hundred meters of Rødvig harbor, along the stretch of coast that runs eastward toward the point at Korsnæb. The height of the cliff is about 12 m. The till layer is relatively thin, and a correspondingly thin buffer (5 m) has been mapped.

Legend	
	Top of limestone
	K-Pg boundary
	Flint band
	Other undercut
	Overhang
	Buffer

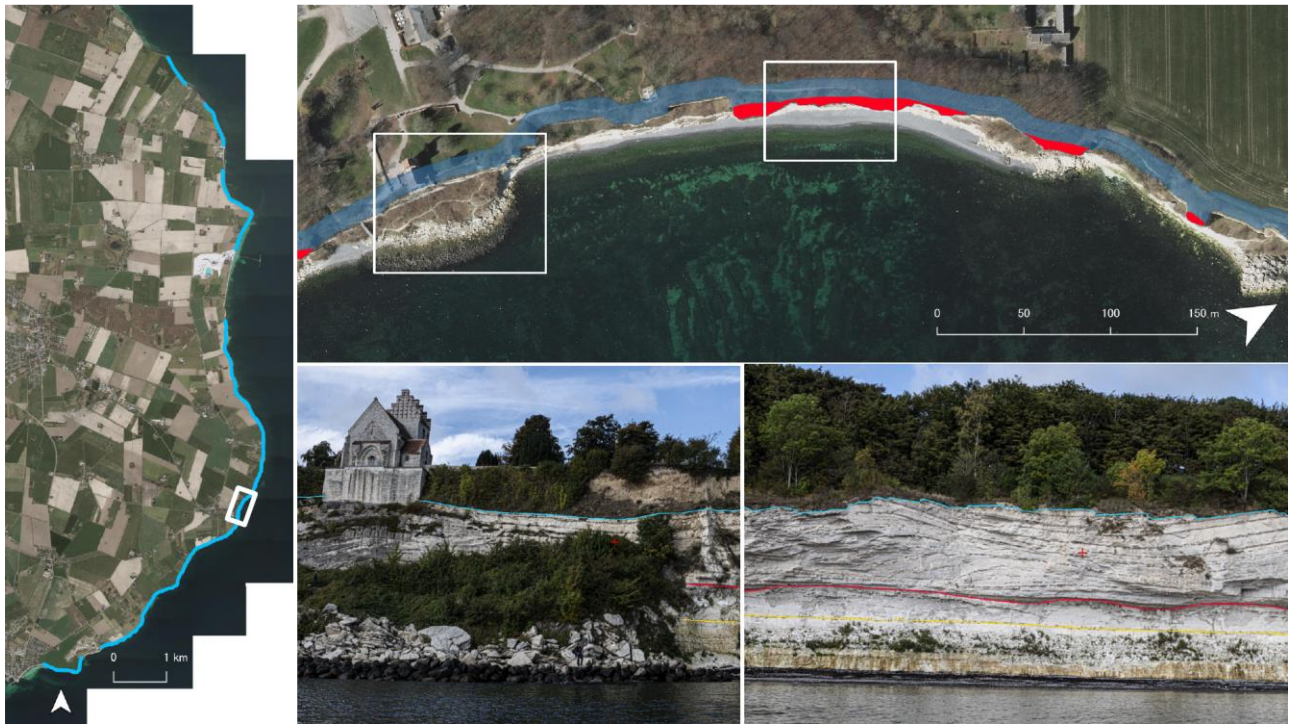
Boesdal



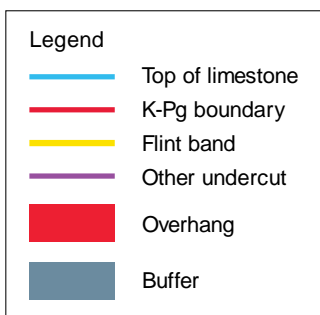
The largest overhangs along the Stevns coastline are found at the caves north of Boesdale quarry. The undercut was digitised at or close to sea level along this stretch. The height of the cliff is about 10 m.



Højerup



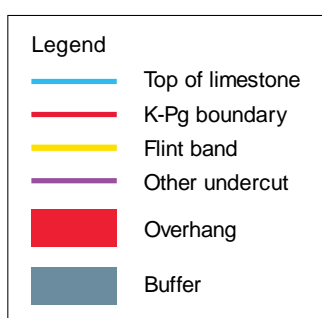
The best documented landslide on the coast is that which claimed the choir of Højerup Old Church in 1928. The Church is now well shielded by the former landslide and defensive boulders. However, immediately to the north the beach passes under a large and well-visited overhang, the southern edge of which coincides with a former quarry wall. The height of the cliff is about 25 m.



Stevns Lighthouse (Stevns Fyr)



Stevns Lighthouse sits above a 50 m collapsed section of cliff. To the south, a much larger landslide, over 150 m wide, lies on the beach, and is partly responsible for a relative lack of overhang on the coast running southwards from the lighthouse. To the north, still-intact overhangs are among the largest along the coast. A thick buffer is applied here to reflect the relatively thick till along this stretch. The height of the cliff is about 40 m.



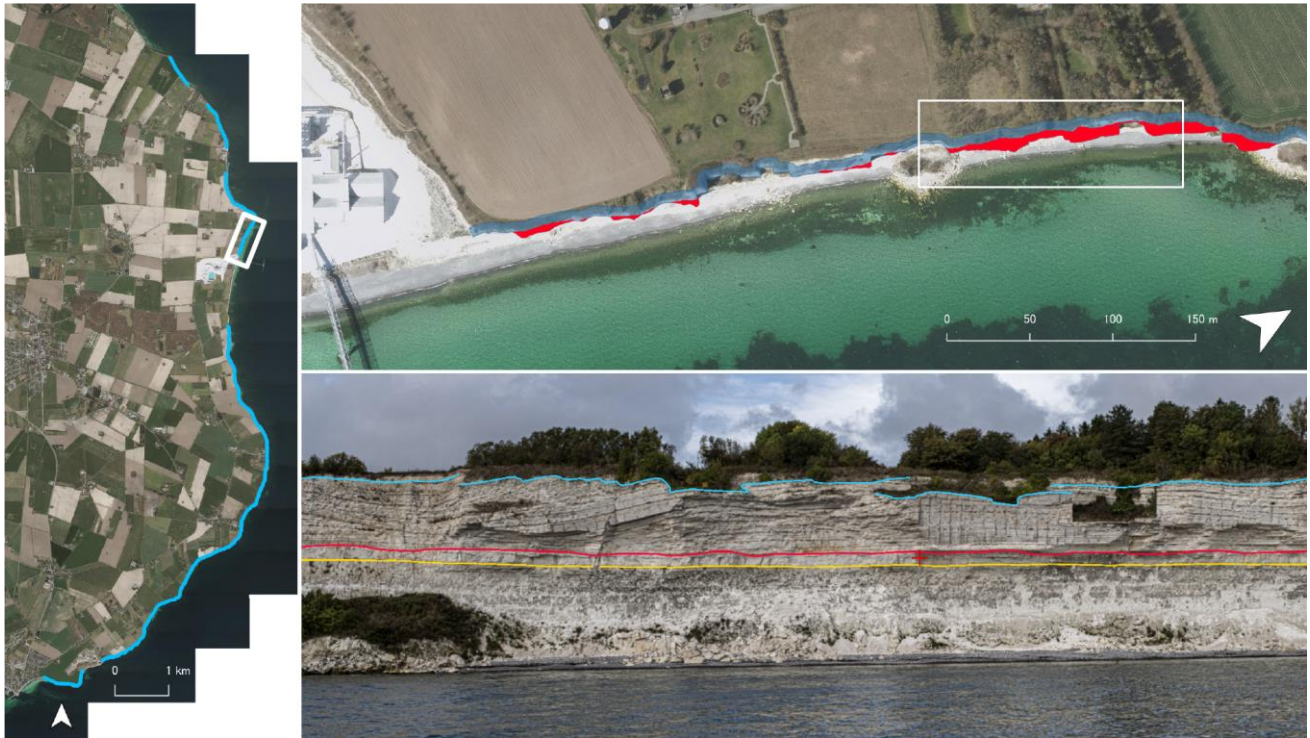
Lilledal



Between Storedal and Sigerslev quarry the K-Pg boundary rises above the present topography, with the result that the cliff is made up of chalk with a cover of till. This composition does not permit the formation of large overhangs, and the absence of past landslides on the beach points to smaller-scale continual erosion predominating. The height of the cliff is about 25 m.

Legend	
—	Top of limestone
—	K-Pg boundary
—	Flint band
—	Other undercut
■	Overhang
■	Buffer

North of Sigerslev quarry



The reappearance of the K-Pg boundary north of Sigerslev quarry instigates the resumption of cliff overhangs. Although the overhangs are large, the till cover is relatively thin, so a correspondingly narrow buffer has been applied. Note the small abandoned quarry (upper right in the lower photograph) causing angular blocks of limestone to protrude over the beach. The height of the cliff is about 35 m.

Legend	
—	Top of limestone
—	K-Pg boundary
—	Flint band
—	Other undercut
■	Overhang
■	Buffer